General two Higgs doublet model (2HDM-G) and Large Hadron Collider data

Yang Bai, Vernon Barger, Lisa L. Everett, and Gabe Shaughnessy

Phys. Rev. D **87**, 115013 — Published 11 June 2013

DOI: 10.1103/PhysRevD.87.115013

General Two Higgs Doublet Model (2HDM-G) and Large Hadron Collider data

Yang Bai[a,b], Vernon Barger[a], Lisa L. Everett,[a] and Gabe Shaughnessy[a]

[a]Department of Physics, University of Wisconsin, Madison, WI 53706, USA
[b]SLAC National Accelerator Laboratory, 2575 Sand Hill Road, Menlo Park, CA 94025, USA

We study the consistency of two Higgs doublet models in light of the new bosonic particle discovery at the LHC. We work within a general setup that we call here the 2HDM-G, in which the quarks couple to both scalar doublets with aligned couplings such that flavor-changing neutral currents are absent at tree level. The framework encompasses the traditional Type I, Type II, lepton specific, and flipped models, but also provides for more general possibilities. The best fit to the current data is given in the general scenario with specific parameter choices; however, a good fit is also obtained within a democratic model in which both the up-type and down-type quarks couple to each doublet with equal strengths. The approach provides a general framework in which to interpret future LHC Higgs data within extensions of the Standard Model with two Higgs doublets.

PACS numbers: 12.60.Fr, 14.80.Ec

Introduction. The recent discovery of a Higgs-like particle with a mass close to 125 GeV at the Large Hadron Collider (LHC) is the most significant crowning achievement in particle physics in several decades. If this particle is indeed a Higgs boson, it is of paramount importance in confirming spontaneous electroweak symmetry breaking as the origin of mass. The properties of the Higgs boson at colliders are also sensitive to physics beyond the Standard Model (SM). Knowing or excluding additional new particles that affect the Higgs properties can increase our understanding of the nature of electroweak symmetry breaking. One of the best-motivated extensions of the SM is to add an additional Higgs doublet, resulting in two Higgs doublet models (2HDM's) (see [1] for a recent review). Specific realizations of 2HDM's have already been studied in light of the Higgs-like particle discovery [2–4].

There are several well-known 2HDM's that correspond to different ways of coupling the Higgs doublets to the SM fermions. The models can be classified into two categories depending on whether they result in Higgs-mediated flavor-changing neutral currents (FCNC) at tree level. Within the first class of models, tree-level FCNC are forbidden by global symmetries such as Peccei-Quinn symmetry [5] or discrete symmetries. This class of models include the Type I (2HDM-I), Type II (2HDM-II), lepton-specific (2HDM-L) and flipped 2HDM, which can be distinguished based on Yukawa coupling measurements [6, 7]. The second class of models, which are commonly known as Type III models, include Yukawa couplings of the up-type and down-type quarks to both Higgs doublets. This class of models generically have tree-level FCNC and are highly constrained by flavor observables which are consistent with the SM.

Motivated by the measurements of the fermion Yukawa couplings and the agreement of the flavor observables with the SM, we explore a simple and relatively general 2HDM framework that captures the dominant effects of Type III models in modifying the Higgs properties but has no tree-level FCNC. In this setup, which we label here for simplicity as the 2HDM-G, the quarks each couple to both Higgs doublets with an aligned flavor structure governed by the same Yukawa matrix, as outlined in [11]. This coupling choice guarantees the absence of tree-level FCNC due to fine-tuning, and therefore FCNC may reappear at higher-loop level with appreciable strength. However, we consider this general framework because our principal guidance is the experimental Higgs data, which points to specific features that are not yet understood.

The 2HDM-G. We consider two complex electroweak Higgs doublets: $\mathbf{\Phi}_d = (\Phi_d^0, \Phi_d^-)$ with hypercharge $Y = -1$, and $\mathbf{\Phi}_u = (\Phi_u^+, \Phi_u^0)$ with $Y = +1$. Assuming that the tree-level Higgs potential conserves CP, we have

$$\begin{aligned} \mathbf{\Phi}_d &= \left[\, (v_d + \phi_d^r + i\,\phi_d^i)/\sqrt{2}\,, \;\; \Phi_d^- \, \right] , \\ \mathbf{\Phi}_u &= \left[\, \Phi_u^+ \,, \;\; (v_u + \phi_u^r + i\,\phi_u^i)/\sqrt{2} \, \right] , \end{aligned} \tag{1}$$

in which $v_{u,d}$ are the usual electroweak vacuum expectation values (VEV's), with $v^2 = v_u^2 + v_d^2 = (246\ \text{GeV})^2$. The ratio of the two VEV's is given by $\tan\beta \equiv v_u/v_d$. Assuming CP conservation, the scalar potential is

$$\begin{aligned} V_\Phi &= m_1^2 \mathbf{\Phi}_d^\dagger \mathbf{\Phi}_d + m_2^2 \mathbf{\Phi}_u^\dagger \mathbf{\Phi}_u - \left(m_{12}^2 \mathbf{\Phi}_d^\dagger \tilde{\mathbf{\Phi}}_u + \text{h.c.} \right) \\ &+ \frac{\lambda_1}{2} |\mathbf{\Phi}_d^\dagger \mathbf{\Phi}_d|^2 + \frac{\lambda_2}{2} |\mathbf{\Phi}_u^\dagger \mathbf{\Phi}_u|^2 + \lambda_3 |\mathbf{\Phi}_d^\dagger \mathbf{\Phi}_d \mathbf{\Phi}_u^\dagger \mathbf{\Phi}_u| \\ &+ \lambda_4 |\mathbf{\Phi}_d^\dagger \tilde{\mathbf{\Phi}}_u \mathbf{\Phi}_u^\dagger \tilde{\mathbf{\Phi}}_d| + \left[\frac{\lambda_5}{2} (\mathbf{\Phi}_d^\dagger \tilde{\mathbf{\Phi}}_u)^2 + \right. \\ &+ \left. \lambda_6 \mathbf{\Phi}_d^\dagger \mathbf{\Phi}_d \mathbf{\Phi}_d^\dagger \tilde{\mathbf{\Phi}}_u + \lambda_7 \mathbf{\Phi}_u^\dagger \mathbf{\Phi}_u \mathbf{\Phi}_d^\dagger \tilde{\mathbf{\Phi}}_u + \text{h.c} \right] , \end{aligned} \tag{2}$$

in which all parameters are real, and $\tilde{\mathbf{\Phi}}_{u,d} \equiv -i\sigma_2 \mathbf{\Phi}_{u,d}^*$. Note that the $\lambda_{6,7}$ terms, which are absent within specific 2HDM's in which there is a softly broken Z_2 symmetry (see e.g. [1] for a review), are generically present within this framework due to the choice of couplings of the Higgs doublets to the quarks, as outlined more precisely below.

In the Higgs spectrum, there are two neutral scalars h and H, one pseudo-scalar A, and one charged scalar $H^\pm$.

We mainly consider the phenomenology of the lightest CP-even neutral scalar h, but we will also include the effects of the charged scalar on the h properties as well as the experimental constraints on H, A and $H^\pm$. The lightest CP-even scalar h is given as usual by $h = -\phi_d^r \sin\alpha + \phi_u^r \cos\alpha$ with the mixing angle $-\pi/2 \leq \alpha < \pi/2$. In the decoupling limit with $m_h \ll m_A \sim m_H \sim m_{H^\pm}$, one has $\cos(\beta-\alpha) = \mathcal{O}(v^2/m_A^2)$ [12]. The tree-level couplings of h to the W and Z are

$$g_{hVV} \;=\; g_V\, m_V\, \sin(\beta-\alpha)\,, \tag{3}$$

in which $g_V = 2m_V/v$ for $V = W$ or Z. The Yukawa couplings of the Higgs doublets to the quarks and the charged leptons are given in this framework without loss of generality as follows:

$$\begin{aligned} -\mathcal{L} \;=\;& y_u\, \overline{u}_R\, (\cos\gamma_u\, \mathbf{\Phi}_u \;-\; \sin\gamma_u\, \tilde{\mathbf{\Phi}}_d)\, Q_L \\ &+ y_d\, \overline{d}_R\, (\cos\gamma_d\, \mathbf{\Phi}_d \;+\; \sin\gamma_d\, \tilde{\mathbf{\Phi}}_u)\, Q_L \\ &+ y_\ell\, \overline{e}_R\, \mathbf{\Phi}_d\, L_L \;+\; \text{h.c.}\,, \end{aligned} \tag{4}$$

in which $y_{u,d,\ell}$ are 3×3 Yukawa matrices, and we have neglected the neutrino interactions with the Higgs for simplicity. In the above, we have used the freedom to redefine the two linear combinations of $\mathbf{\Phi}_u$ and $\tilde{\mathbf{\Phi}}_d$ [13] to eliminate the coupling of the leptons to $\tilde{\Phi}_u$. Hence, in this basis there are two mixing angles $\gamma_{u,d}$ for the up-type and down-type quark couplings.

Type	I	II	L	Flipped	Democratic
γ_u	$\frac{\pi}{2}$	0	0	$\frac{\pi}{2}$	$\frac{\pi}{4}$
γ_d	0	0	$\frac{\pi}{2}$	$\frac{\pi}{2}$	$\frac{\pi}{4}$

TABLE I: The values of the mixing angles $\gamma_{u,d}$ for different 2HDM's. "L" means the lepton-specific 2HDM (2HDM-L). The flipped 2HDM is similar to the 2HDM-II except that the charged leptons couple to the same Higgs as the up-type quarks. The democratic (2HDM-D) refers to the case in which both doublets couple equally to up and down quarks.

In specific limits, the parameter space of this scenario reduces to several well-known 2HDM's, as shown in Table I. It is clear that this more general framework will allow us to cover a broader range in the Higgs sector than any of these familiar limits. The couplings of h to fermions, in units of the SM coupling, take the form

$$\begin{aligned} h t\bar{t}: &\quad \frac{\cos(\alpha+\gamma_u)}{\sin(\beta+\gamma_u)}\,, \qquad h b\bar{b}: \quad -\frac{\sin(\alpha-\gamma_d)}{\cos(\beta-\gamma_d)}\,, \\ h\tau\bar{\tau}: &\quad -\frac{\sin\alpha}{\cos\beta}\,, \end{aligned} \tag{5}$$

in which we have shown only the dominant tree-level couplings to the third-generation fermions. The Yukawa couplings involving the charged Higgs $H^\pm$ are given by

$$\begin{aligned} g_{H^- t\bar{b}} \;&=\; \frac{\sqrt{2}}{v}\left[m_t \cot(\beta+\gamma_u)\, P_R + m_b \tan(\beta-\gamma_d)\, P_L\right], \\ g_{H^-\tau^+\nu} \;&=\; \frac{\sqrt{2}}{v}\left[m_\tau \tan\beta\, P_L\right], \end{aligned} \tag{6}$$

which corresponds to (in commonly used notation) $A_u \equiv \cot(\beta+\gamma_u)$ and $A_d \equiv \tan(\beta-\gamma_d)$.

We see from Eqs. (3) and (5) that the SM Higgs boson couplings are recovered by choosing $\beta = \alpha + \pi/2$ and $\gamma_u = \gamma_d = 0$. The couplings to the electroweak gauge bosons are generically smaller in this general setup than their SM values. However, the couplings to fermions can be either larger or smaller than the corresponding SM couplings. Also, unlike the discrete 2HDM's, the couplings to the t-quark, the b-quark and the τ-lepton are independent of each other. For example, by choosing $\alpha = 0$ and nonzero values of γ_u and γ_d, one can even have a vanishing $h \to \tau\bar{\tau}$ partial decay width.

To compare with the experimental measurements, it is necessary to determine the branching fractions of various Higgs decay channels in this setup. First, we determine the total width of h, which is given by

$$\Gamma_h^{\rm tot} \approx \frac{\sin^2(\alpha-\gamma_d)}{\cos^2(\beta-\gamma_d)}\,\Gamma_{\rm SM}^b \;+\; \sin^2(\beta-\alpha)\,\Gamma_{\rm SM}^W\,, \tag{7}$$

where for illustrative purposes we have assumed that the total width is always dominated by the $b\bar{b}$ and W^+W^- channels and thus we have neglected subdominant contributions from $\tau\tau$ and gg. In our numerical calculations, we include all the subdominant channels in the determination of the total width. Given the parameter space freedom, the total width can be much larger or smaller than the total width of the SM Higgs boson. The ratio of branching ratios for several important channels, $\rho_i \equiv {\rm BF}_i(2{\rm HDM_X})/{\rm BF}_i({\rm SM})$, then take the form

$$\rho_g \;=\; \frac{\cos^2(\alpha+\gamma_u)}{\sin^2(\beta+\gamma_u)}\frac{\Gamma_{\rm SM}^{\rm tot}}{\Gamma_{\rm X}^{\rm tot}}\,,\; \rho_b = \frac{\sin^2(\alpha-\gamma_d)}{\cos^2(\beta-\gamma_d)}\frac{\Gamma_{\rm SM}^{\rm tot}}{\Gamma_{\rm X}^{\rm tot}}\,, \tag{8}$$

$$\rho_\tau \;=\; \frac{\sin^2\alpha}{\cos^2\beta}\frac{\Gamma_{\rm SM}^{\rm tot}}{\Gamma_{\rm X}^{\rm tot}}\,, \qquad \rho_V = \sin^2(\beta-\alpha)\frac{\Gamma_{\rm SM}^{\rm tot}}{\Gamma_{\rm X}^{\rm tot}}\,, \tag{9}$$

$$\rho_\gamma \;=\; \left[\frac{16\cos(\alpha+\gamma_u)}{47\sin(\beta+\gamma_u)} - \frac{63\sin(\beta-\alpha)}{47}\right]^2 \frac{\Gamma_{\rm SM}^{\rm tot}}{\Gamma_{\rm X}^{\rm tot}}\,. \tag{10}$$

For ρ_γ, we show here the result in the limit $m_h \ll 2m_t, 2M_W$, but in our numerical calculations we use the full one-loop formula including the $H^\pm$ contribution [14, 15].

The data are typically presented as ratios of the production cross section times branching fraction divided by the corresponding SM value, with the notation $\mu_j(i)$ for the production type "i" and the decay channel "j." The $\mu_j(i)$ can be related to the ρ_i by $\mu_j(i) = \rho_j\,\rho_i$ for the exclusive channel. For the inclusive channel, we sum over the gg, VV and Vh production modes.

Fit to the Higgs data. We perform a Bayesian fit to the available LHC and Tevatron data following the same method as [16]. We require all scalar potential parameters to be perturbative with $\lambda_i^2 < 4\pi$. We have also included constraints on the parameter space that result from the requirement that the potential is bounded from

below [17], and from vacuum stability (see [18] for a general discussion of this issue in CP-conserving 2HDM's).

From the present experimental results as of Moriond 2013 [9, 10, 19, 21–23] (see also [8]), a combination of inclusive and selected exclusive channels yields the following distilled measurements:

$$\begin{aligned}
\mu_{gg}(\gamma\gamma) &= 1.1^{+0.2}_{-0.2}\,, \quad \mu_{VV}(\gamma\gamma) = 1.2^{+0.5}_{-0.5}\,, \\
\mu_{gg}(VV) &= 0.79^{+0.15}_{-0.15}\,, \quad \mu_{VV}(VV) = 1.0^{+0.4}_{-0.4}\,, \\
\mu_{gg}(\tau\tau) &= 0.9^{+0.6}_{-0.5}\,, \quad \mu_{VV}(\tau\tau) = 1.3^{+0.6}_{-0.6}\,, \\
\mu_{Vh}(b\bar{b}) &= 1.3^{+0.4}_{-0.4}\,,
\end{aligned}$$

where pp, gg, VV and Vh denote inclusive, gluon fusion, vector boson fusion and associated production of the Higgs boson. We constrain H with the excluded signal rate over a mass range up to 500 GeV [19] and $H^{\pm}$ with a mass below the top mass [20], in accordance with current limits. We also include the values of the precision electroweak observables S and T and the flavor changing decays $B^0 \to X_s + \gamma + X$ at next to leading order (NLO) [24] in our fit. We require $S = 0.04 \pm 0.09$, $T = 0.07 \pm 0.08$ with an 88% positive correlation [25] and $\mathrm{BF}(B^0 \to X_s + \gamma + X) = (3.43 \pm 0.22) \times 10^{-4}$ [26].[1]

The $B^0 \to X_s + \gamma + X$ measurement places a significant constraint on the charged Higgs couplings. We show in Fig. 1 the plane of A_u and A_d for two charged Higgs masses and the associated regions of the traditional 2HDMs. Models that allow a simultaneous suppression of A_u and A_d, such as the 2HDM-I, 2HDM-L, and 2HDM-D models, better permit a light charged Higgs. The 2HDM-II and flipped models require a rather heavy charged Higgs to evade the current bounds.

In Fig. 2, we show the bands associated with the collider measurements of Eq. (11) in $\cos(\beta - \alpha)$ and $\tan\beta$ for 2HDM-D. The solid lines indicate the central value while the shaded region indicates the 1σ band of the measurements combined over all production channels [$\mu(VV) = 0.8^{+0.1}_{-0.1}$, $\mu(\gamma\gamma) = 1.1^{+0.2}_{-0.2}$, $\mu(b\bar{b}) = 1.3^{+0.4}_{-0.4}$ and $\mu(\tau\tau) = 1.1^{+0.4}_{-0.4}$]. The Bayesian fit is represented by the red points. Therefore, the measured VV, $\gamma\gamma$ and $\tau\tau$ rates provide a good fit for small $\tan\beta$ and $\cos(\beta - \alpha) \to 0$, in accordance with the decoupling limit and $B^0 \to X_s + \gamma + X$.

In Fig. 3, we show the posterior mass distribution of the heavy states, which have the peak values different from the decoupling limit. Note that it is difficult to get such a large $b\bar{b}$ value of $\mu_{Vh}(b\bar{b}) = 1.3$ indicated by the data. This is due to the already large branching fraction in the SM. Hence, no central value line is shown for that channel. However, this large value is dominated by the Tevatron $Vh \to b\bar{b}$ measurement. If the future rate measured at the LHC is smaller as indicated by the CMS measurement, agreement within this channel will improve. With a suppressed $b\bar{b}$ rate, another means to enhance the $h \to \gamma\gamma$ rate is available as the total width decreases, thereby increasing the branching fraction to the other decay modes. We find this occurs infrequently within this scenario.

In Fig. 4, we show the posterior probability density

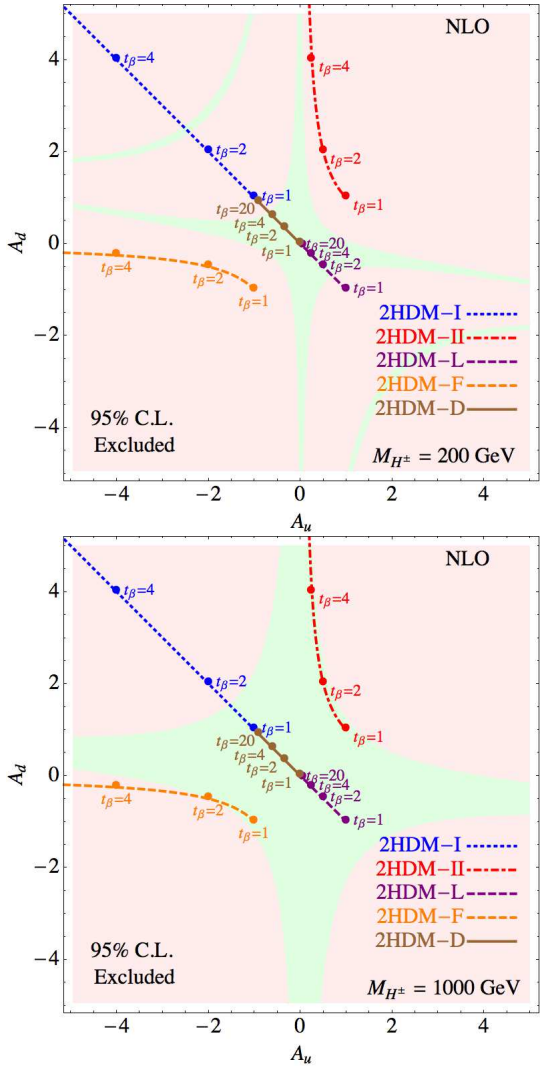

FIG. 1: Allowed regions consistent with $B^0 \to X_s + \gamma + X$ measurements in A_u and A_d for $M_{H^\pm} = 200$ GeV and 1 TeV. Traditional models that allow a suppression in both A_u and A_d are favored when the charged Higgs boson is light. For each traditional model, we illustrate the location for a selected set of $\tan\beta$ values. Pink regions denote exclusion at the 95% C.L.

[1] The BaBar collaboration has reported measurements of $B \to D^+(D*^+)\tau^-\nu$ that deviate from Standard Model predictions by 2σ and 2.7σ, respectively [27]. In the context of a 2HDM these measurements appear to require a charged Higgs with mass below the LEP2 limit. In the BaBar analyses only the purely leptonic tau decay modes are studied and the presence of multiple neutrinos in the final state requires complex methodology to separate the signals from backgrounds. Hence, we set aside the BaBar results until independent measurements of these decay modes are reported by the Belle and LHCb collaborations.

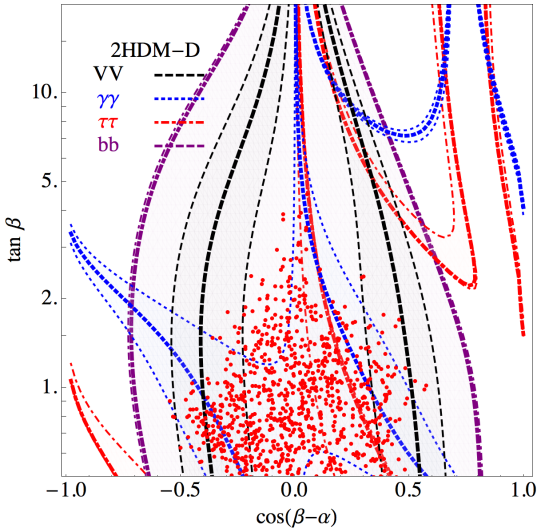

FIG. 2: Ranges of $\cos(\beta-\alpha)$ and $\tan\beta$ in 2HDM-D consistent with the experimental data. Data consisting of decays to VV, $\gamma\gamma$, $\tau\tau$ and $b\bar{b}$ constrain the parameter space to regions of black, blue, red, and purple colors, respectively. A random selection of points in our Bayesian fit are presented as red dots. Due to $B^0 \to X_s + \gamma + X$ constraints, models with small $\tan\beta$ are preferred.

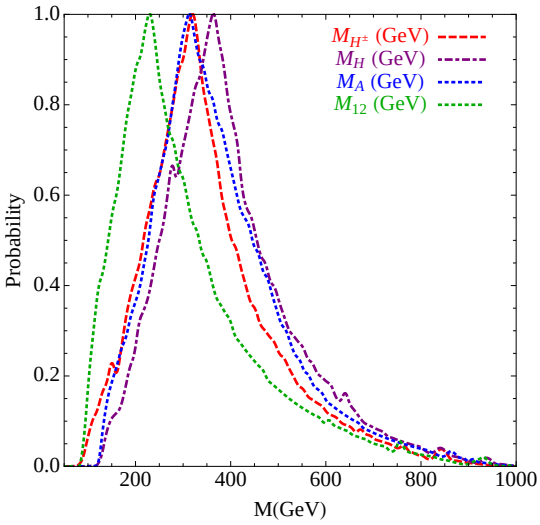

FIG. 3: Posterior probability of the heavy Higgs masses. To achieve the enhanced $h \to \gamma\gamma$ rate, the charged Higgs is typically light. Consistency with electroweak precision observables forces the associated heavy states to be of similar mass.

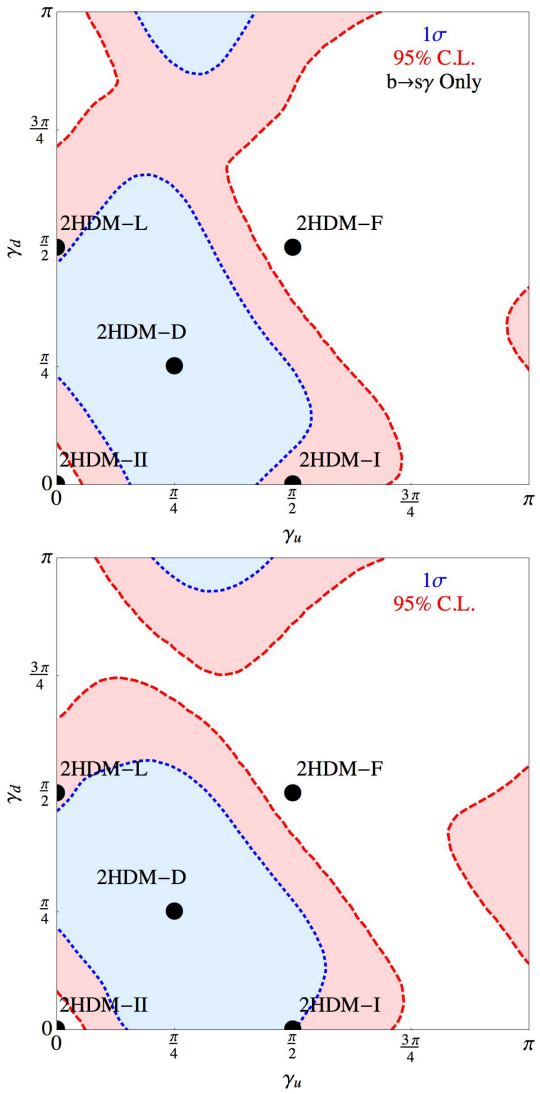

FIG. 4: Posterior probability regions of 1σ and 95% C.L. in the plane of γ_u and γ_d consistent with only $B^0 \to X_s + \gamma + X$ (top panel) and all data (bottom panel). Traditional 2HDM models (black circles) and the 2HDM-D (middle black circle) are shown for comparison.

in the plane of γ_u and γ_d considering only $B^0 \to X_s + \gamma + X$ (top panel) and including all the data (bottom panel). The dominant constraint in this plane arises from $B^0 \to X_s + \gamma + X$. The LHC and EW precision data continue to carve out more of the available parameter space. The most preferred values do not fit any of the traditional models. Of these models, the 2HDM-II and flipped models have the most tension from $B^0 \to X_s + \gamma + X$ as they lie outside the 95% C.L. region. This is verified by the best-fit reduced χ^2 distribution by channel tabulated in Table II. (The best fit point for the general model does not necessarily correspond to the most likely point due to the sampling of the parameter space; for instance, a fine-tuned best fit point is generally not the most likely point.) The values of $\gamma_u = \gamma_d = \pi/4$ appear to give quite good fits for the democratic 2HDM-D model.

As shown in Table II, the best fit is given by the general setup with specific parameter choices, with the 2HDM-D not far behind. The pull from the data of the best fits are given in Fig. 5, which immediately shows that the data are well matched for specific parameter

TABLE II: Reduced χ^2 values of the best fit point for key channels. For each Higgs decay channel, we sum over the production mechanisms.

Model	χ^2_{VV}/ν	$\chi^2_{\gamma\gamma}/\nu$	$\chi^2_{b\bar{b}}/\nu$	$\chi^2_{\tau\tau}/\nu$	$\chi^2_{b\to s\gamma}$	$\chi^2_{\rm total}/\nu$
SM	0.45	0.91	1.00	0.27	0.17	0.65
Type-I	0.52	0.76	1.13	0.32	0.06	0.60
Type-II	0.49	0.92	1.00	0.26	2.78	0.71
Lepton	0.62	0.77	0.99	0.27	0.02	0.55
Flipped	0.52	0.93	0.99	0.29	2.49	0.72
Democratic	0.43	0.76	1.22	0.31	0.00	0.59
General	0.44	0.77	0.99	0.27	0.02	0.55

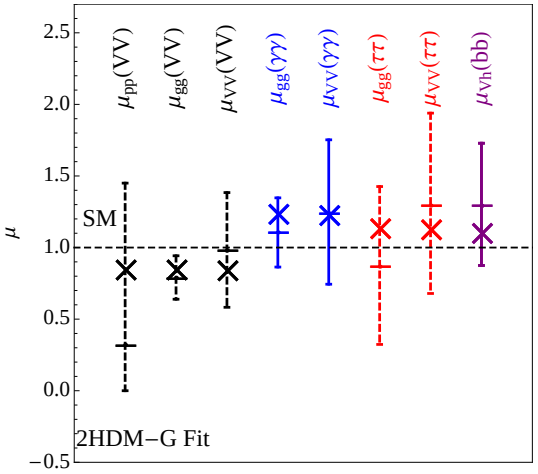

FIG. 5: Channels measured at the LHC and Tevatron with best fit points from the 2HDM-G model denoted by ×.

regions within this general 2HDM framework.

Conclusions. The 2HDM-G framework provides a rich setting in which to analyze the LHC Higgs-like data in the context of simple extensions of the SM to allow for two electroweak Higgs doublets. As one might expect, the general model provides the best fit to the current data, with the democratic model not far behind. A charged Higgs of moderate mass is common. Further measurements of the neutral Higgs boson properties and searches for the charged Higgs boson will verify or falsify models within this framework.

We note here that during the completion of our paper, another paper appeared that also analyzes general two Higgs doublet models with vanishing tree-level FCNC's, with a different parametrization [29].

Acknowledgments. We thank Daniel Chung for useful discussions. VB, LE, and GS are supported by the U. S. Department of Energy under the contract DE-FG-02-95ER40896. YB is supported by start-up funds from the Univ. of Wisconsin, Madison. YB thanks SLAC for warm hospitality.

[1] G. C. Branco, P. M. Ferreira, L. Lavoura, M. N. Rebelo, M. Sher and J. P. Silva, Phys. Rept. **516**, 1 (2012) [arXiv:1106.0034 [hep-ph]].
[2] N. Craig and S. Thomas, JHEP **1211**, 083 (2012) [arXiv:1207.4835 [hep-ph]].
[3] D. S. M. Alves, P. J. Fox and N. J. Weiner, arXiv:1207.5499 [hep-ph].
[4] S. Chang, S. K. Kang, J. -P. Lee, K. Y. Lee, S. C. Park and J. Song, arXiv:1210.3439 [hep-ph].
[5] R. D. Peccei and H. R. Quinn, Phys. Rev. Lett. **38**, 1440 (1977).
[6] V. Barger, H. E. Logan and G. Shaughnessy, Phys. Rev. D **79**, 115018 (2009) [arXiv:0902.0170 [hep-ph]].
[7] J. L. Diaz-Cruz, A. Diaz-Furlong and J. H. Montes de Oca, arXiv:1010.0950 [hep-ph].
[8] G. Bernardi and M. Herndon, arXiv:1210.0021 [hep-ex].
[9] [ATLAS Collaboration], ATLAS-CONF-2013-034.
[10] [CMS Collaboration], CMS-PAS-HIG-13-005.
[11] A. Pich and P. Tuzon, Phys. Rev. D **80**, 091702 (2009) [arXiv:0908.1554 [hep-ph]].
[12] J. F. Gunion and H. E. Haber, Phys. Rev. D **67**, 075019 (2003) [hep-ph/0207010].
[13] S. Davidson and H. E. Haber, Phys. Rev. D **72**, 035004 (2005) [Erratum-ibid. D **72**, 099902 (2005)] [hep-ph/0504050].
[14] J. F. Gunion, H. E. Haber, G. L. Kane and S. Dawson, *The Higgs Hunter's Guide*, Westview Press, 2001.
[15] V. D. Barger, M. S. Berger, A. L. Stange and R. J. N. Phillips, Phys. Rev. D **45**, 4128 (1992).
[16] I. Low, J. Lykken and G. Shaughnessy, Phys. Rev. D **86**, 093012 (2012) [arXiv:1207.1093 [hep-ph]].
[17] N. G. Deshpande and E. Ma, Phys. Rev. D **18**, 2574 (1978).
[18] A. Barroso, P. M. Ferreira, I. P. Ivanov and R. Santos, arXiv:1303.5098 [hep-ph].
[19] G. Aad *et al.* [ATLAS Collaboration], Phys. Rev. D **86**, 032003 (2012) [arXiv:1207.0319 [hep-ex]]; Phys. Lett. B **716**, 1 (2012) [arXiv:1207.7214 [hep-ex]].
[20] G. Aad *et al.* [ATLAS Collaboration], JHEP **1206**, 039 (2012) [arXiv:1204.2760 [hep-ex]].
[21] S. Chatrchyan *et al.* [CMS Collaboration], Phys. Lett. B **716**, 30 (2012) [arXiv:1207.7235 [hep-ex]].

[22] [CMS Collaboration], CMS PAG HIG-12-020; CMS PAG HIG-12-015; CMS PAG HIG-12-018.
[23] [Tevatron New Physics Higgs Working Group and CDF and D0 Collaborations], arXiv:1207.0449 [hep-ex].
[24] M. Ciuchini, G. Degrassi, P. Gambino and G. F. Giudice, "Next-to-leading QCD corrections to B $\to$ X(s) gamma: Standard model and two Higgs doublet model," Nucl. Phys. B **527**, 21 (1998) [hep-ph/9710335].
[25] J. Beringer *et al.* [Particle Data Group Collaboration], Phys. Rev. D **86**, 010001 (2012).
[26] Heavy Flavor Averaging Group Collaboration. http://www.slac.stanford.edu/xorg/hfag/rare/2012/radll/btosg.pdf
[27] J. P. Lees *et al.* [BaBar Collaboration], Phys. Rev. Lett. **109**, 101802 (2012) [arXiv:1205.5442 [hep-ex]].
[28] [LEP Higgs Working Group for Higgs boson searches and ALEPH and DELPHI and L3 and OPAL Collaborations], hep-ex/0107031.
[29] W. Altmannshofer, S. Gori and G. D. Kribs, Phys. Rev. D **86**, 115009 (2012) [arXiv:1210.2465 [hep-ph]].